THE JOURNAL OF PHYSICAL CHEMISTRY B

Article

pubs.acs.org/JPCB

Novel Polypropylene/Inorganic Fullerene-like WS_2 Nanocomposites Containing a β-Nucleating Agent: Isothermal Crystallization and Melting Behavior

Mohammed Naffakh,* Carlos Marco, and Gary Ellis

Instituto de Ciencia y Tecnología de Polímeros, ICTP-CSIC, c/Juan de la Cierva, 3, 28006 Madrid, Spain

ABSTRACT: The isothermal crystallization and subsequent melting behavior of isotactic polypropylene (iPP) nucleated with different nucleating agents (NAs) are investigated. Tungsten disulfide (IF-WS_2) and *N,N′*-dicyclohexyl-2,6-naphthalene (NJ) and dual-additive mixtures are introduced into an iPP matrix to generate new materials that exhibit variable α- and β-polymorphism. As shown in previous work, small amounts of IF-WS_2 or NJ have a nucleating effect during the crystallization of iPP. However, the isothermal crystallization and melting behavior of iPP nucleated by dual α(IF-WS_2)/β(NJ) additive systems are dependent on both the NA composition balance and the crystallization temperature. In particular, our results demonstrate that it is possible to obtain any α-phase to β-phase content ratio by controlling the composition of NAs under appropriate isothermal crystallization conditions. The nucleating behavior of the additives can be illustrated by competitive nucleation, and the correlation between crystallization and melting temperatures and relative α- and β-crystals content in iPP in the nanocomposites is discussed.

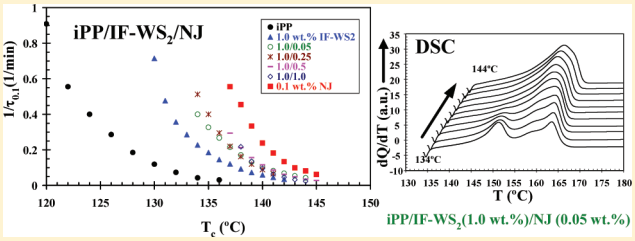

1. INTRODUCTION

Addition of nucleating agents (NAs) directly into bulk of plastic resins during processing has attracted great scientific and industrial attention for several decades and substantial effort continues to be devoted to of this area of research. Many practices in this field are driven by industrial needs to either modify the thermal, mechanical, optical, and/or rheological behavior of the polymer involved or simply reduce the cost.[1−5] In particular, in polymer crystallization a heterogeneous nucleating agent must provide the largest solid surface area, or as many nucleation sites that can nucleate the polymer crystals, as possible and, by defect, must be well dispersed. A low surface free energy of the agent in contact with the polymer melt will allow good wetting of the additive. Crystalline structures or surface features of the additive that are geometrically similar to the polymer crystal structure may promote epitaxial growth and represents the most important mechanism for initiating crystal formation.[6] Other mechanisms of action of nucleating agents such as self-seeding (i.e., nucleation on crystal remains due to partial melting of primary crystals)[7] or chemical reaction (e.g., sodium benzoate reacts as a true chemical reagent with the molten macromolecules and produces ionic end groups which constitute the true nucleating species)[8] have also been reported. Naturally, the agent should be in the solid state in the polymer melt at the temperature at which polymer nucleation takes place and has sufficient thermal stability in order not to limit the processing window of the material. Recently, nanometric fillers have gained some attention due to the remarkable improvement in some materials properties when compared to the virgin polymer or conventional microcomposites. Because of the large specific surface area of nanoparticles that leads to strong interfacial interactions with the surrounding polymer matrix, nanoscaled particles are believed to be more effective for the improvement of the ultimate physical properties, which are tremendously affected by the crystallization of the polymer matrix.[9−11]

Isotactic polypropylene (iPP) is a polymorphic material with four different crystal modifications, comprising of the monoclinic (α), trigonal (β), orthorhombic (γ), and metastable mesomorphic forms.[12−17] The α modification is thermodynamically stable and under processing conditions habitually employed commercial iPP materials mostly crystallize in this form. The addition of specific agents that nucleate the α-crystal form can enhance the tensile and flexural properties as well as transparency of iPP. The β-form is thermodynamically metastable and can only be obtained under special conditions such crystallization in a temperature gradient,[18,19] flow-induced crystallization,[20−24] or the addition of specific β-nucleating agents[25−34] that can improve impact strength and heat distortion temperature of iPP, albeit at the expense of stiffness.[35−39] The β-form exhibits improved elongation at break and excellent impact strength, especially at low temperatures, which can be attributed to the $\beta-\alpha$ polymorphic transition and the less dense structure of β-crystals, compared to α-crystals, that favors the absorption of impact energy.[22,40] The metastable mesomorphic form of iPP can be obtained by very fast cooling of the polymer from the melt and, together

Received: October 17, 2011
Revised: January 18, 2012
Published: January 18, 2012

with the γ-form, can be considered to be relatively rare in processed materials.[16,17,41−43]

As mentioned above, the α-crystals usually present in industrial products prepared by conventional processing techniques have inferior toughness. To date, four approaches have been proposed to improve the toughness of iPP, including copolymerization with other olefin monomers,[44] blending with rubber or thermoplastic elastomer,[45] compounding with organic or inorganic fillers including nanoparticles,[46,47] and addition of β-nucleating agents.[25−34] In this respect, the combination of dual α/β nucleating agents[48−53] can allow the controlled adjustment of stiffness and toughness of iPP and has been demonstrated recently using both micrometer- and nanoscale-size particles[52] as well as various nanoparticles with different form factor and characteristics.[53]

Inorganic fullerenes based on tungsten disulfide (IF-WS_2) nanoparticles have been demonstrated to be effective in inducing the formation of the α-crystal form and very efficiently improve the thermal and mechanical properties of iPP.[54] On the other hand, *N,N′*-dicyclohexyl-2,6-naphthalene dicarboxamide (NJ) is one of the most highly effective third-generation NAs for inducing the formation of the β-crystal form of iPP.[26] When these agents are combined as dual NAs, denominated α(IF-WS_2) and β(NJ), to prepare new materials, under the appropriate dynamic conditions the results obtained have shown that the cooling rate and β(NJ) content are very efficient in controlling the dynamic crystallization behavior and the final crystalline structures of nucleated iPP.[55]

The objective of this work is to investigate the isothermal crystallization and melting behavior of nucleated iPP comparing single additive systems, α(nano) and β(micro), with dual additive systems, α(IF-WS_2)/β(NJ), and study the nucleation effect of both the α- and β-phase NAs, with a view to controlling the crystalline structure of iPP through tuning the crystallization conditions and composition using dual NA systems.

2. EXPERIMENTAL SECTION

2.1. Materials and Processing. Isotactic polypropylene (iPP) was provided by Repsol-YPF (Móstoles, Spain), with 95% isotacticity, a viscosity average molecular weight of 179 000 g/mol,[56] and a polydispersity of 4.77. The IF-WS_2 nanoparticles (NanoLub) were kindly supplied by Nanomaterials (Israel, known as ApNano Materials in the USA). The IF-WS_2 nanoparticles are multifaceted polyhedra with an apparent shape ranging from spheres to ellipsoids. The particle aspect ratio ranges between 1 (spheres) and 2.3, with a mean value of 1.4, a standard deviation of 0.3, and a median of 1.36. The particle dimensions are in the range of 40−200 nm with a mean value of 80 nm, standard deviation of 30 nm, and median of 75 nm.[54] The β-nucleating agent used was *N,N′*-dicyclohexyl-2,6-naphthalene dicarboxamide (NJSTAR NU100), denominated NJ, kindly provided by RIKA International LTD (Manchester, UK).

Several concentrations of dual IF-WS_2/NJ additive systems were introduced into the iPP matrix by melt-mixing for 15 min using a Thermo-Haake Minilab microextruder operated at 210 °C with a rotor speed of 150 rpm. The NJ concentrations were 0.05, 0.25, 0.5, and 1.0 wt %, while the IF-WS_2 content was always 1.0 wt % (i.e., IF-WS_2/NJ = 1.0/0.05, 1.0/0.25, 1.0/0.50, and 1.0/1.0 wt %/wt %). With the aim of improving the dispersion of the nanoparticles and β-nucleating agent in the matrix, IF-WS_2 was first introduced into the iPP matrix and mixed for 10 min, according to previous work.[54] Subsequently, NJ was introduced into the extruder and mixing continued for another 5 min. Also, samples of neat iPP and binary systems of iPP/IF-WS_2 (1.0 wt %) and iPP/NJ (0.1 wt %) were prepared under the same conditions.

2.2. Characterization Techniques. *2.2.1. Differential Scanning Calorimetry (DSC).* The crystallization and melting experiments were carried out with a Perkin-Elmer DSC7-7700 differential scanning calorimeter (Perkin-Elmer España SL, Madrid, Spain), calibrated with indium (T_m = 156.6 °C, ΔH_m = 28.45 kJ/kg) and zinc (T_m = 419.47 °C, ΔH_m = 108.37 kJ/kg). Aluminum capsules were used with sample weights of ∼10 mg studied under an inert nitrogen atmosphere flow at a rate of 25 mL/min. The thermal history prior to crystallization of iPP was controlled by maintaining the samples in the melt for 5 min at a residence temperature of 210 °C, eliminating memory effects, and assuring the maximum thermal stability of the components.[57] Subsequently, the samples were cooled from the melt to each isothermal crystallization temperature (T_c) at a rate of 64 °C/min, and the crystallization exotherm registered as a function of time until crystallization was considered to be complete. The time associated with each transformation level (τ_i) was obtained by integration of the corresponding crystallization exotherms. The crystallization rate was analyzed using values of $\tau_{0.1}$ that correspond to the time required to reach a crystalline transformation level of 10%. Considering crystalline rate ∼ $(1/\tau_{0.1})$, this parameter represents the overall crystallization rate for each crystallization temperature. After crystallization was completed, the melting temperatures (T_m) were determined by heating the samples at a rate of 5 °C/min, and the enthalpies corresponding to the α-crystal form ($T_{m,\alpha}$) and β-crystal form ($T_{m,\beta}$) were calculated according to the method recommended by Li and Cheung[58] employing PeakFit software (Systat Software GmbH, Erkrath, Germany) to obtain the contributions of the α and β melting peaks in the complex thermograms. The crystallinity of the α-form, X_α, and β-form, X_β, and the β-form content (k_β) were calculated as follows:

$$X_\alpha = \frac{\Delta H_\alpha}{\Delta H^0_{m,\alpha}} \quad (1)$$

$$X_\beta = \frac{\Delta H_\beta}{\Delta H^0_{m,\beta}} \quad (2)$$

$$k_\beta = \frac{\Delta H_\beta}{\Delta H_\alpha + \Delta H_\beta} \quad (3)$$

where $\Delta H^0_{m,\alpha}$ is the enthalpy fusion of 100% crystalline α-iPP, taken as 177 J/g, and $\Delta H^0_{m,\beta}$ is the enthalpy of 100% crystalline β-iPP, taken as 168.5 J/g.[59]

3. RESULTS AND DISCUSSION

The isothermal crystallization behavior of neat iPP has been analyzed over a crystallization temperature range between 120 and 136 °C. Figure 1a shows the evolution of the crystallization exotherms of iPP. As the crystallization temperature increased, the exotherms shifted along the time axis. Both the induction time and the width of the exotherms increased, reflecting a reduction in the crystallization rate with decreasing undercooling of the system, ΔT. When IF-WS_2 was introduced into iPP (Figure 1b), the crystallization rate was greatly enhanced, demonstrated by an important shift of the practically attainable

dx.doi.org/10.1021/jp2099703 | J. Phys. Chem. B 2012, 116, 1788−1795

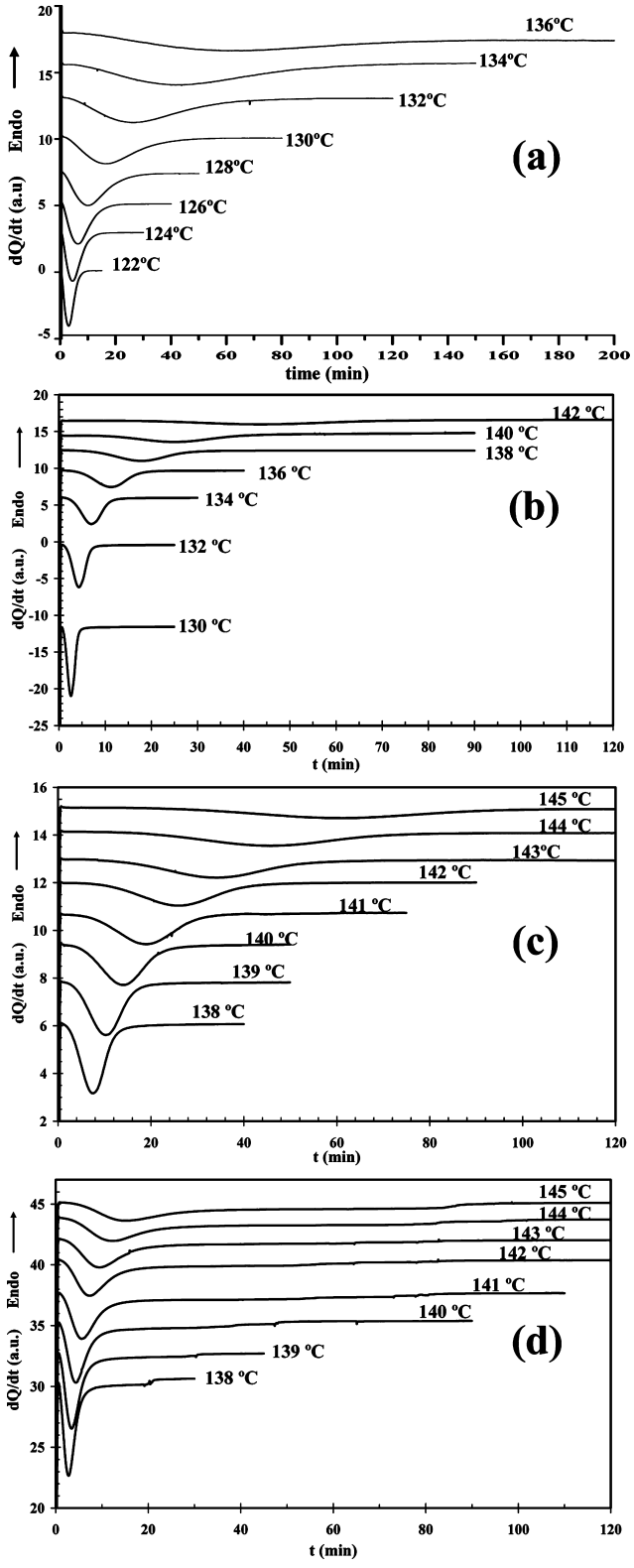

Figure 1. DSC thermograms of isothermal crystallization of (a) iPP, (b) iPP/IF-WS_2 (1.0 wt %), (c) iPP/IF-WS_2 (1.0 wt %)/NJ(1.0 wt %), and (d) iPP/NJ(0.1 wt %) obtained at the indicated crystallization temperatures.

crystallization range of iPP by over 10 °C, from 130 to 142 °C. This is directly related to the high nucleating effect of the IF-WS_2 nanoparticles on the monoclinic α-crystal form of iPP.[60] In the iPP/IF-WS_2/NJ systems, the addition of β(NJ) exerted a significant effect on the crystallization of iPP. Similarly, increasing the crystallization temperature resulted in a more apparent difference in the crystallization rates between iPP/IF-WS_2/NJ and iPP/IF-WS_2. Clearly, for iPP nucleated with α(IF-WS_2)/β(NJ), the nucleating effect was higher than the iPP/IF-WS_2 system but remained lower than the iPP/NJ system (Figure 1c,d). The crystallization exotherms for iPP/NJ presented shorter induction times and a narrower peak width than those observed for the iPP/IF-WS_2/NJ systems. In particular, an interesting exothermic peak-doubling phenomenon occurred in the iPP/NJ sample containing 0.1 wt % of NJ (Figure 1d). The second peak that is broad and not particularly evident was not detected in neat iPP or in iPP/IF-WS_2/NJ systems and may be an indication of separated growth of the α- and β-phases. Vychopnová et al.[30] also found similar multiple exothermic characteristic in the thermograms when iPP was nucleated using 0.01 mass % of NJ isothermally crystallized at a higher temperature of 140 °C. The author assigned the appearance of such behavior to the formation of a peculiar $\beta\alpha$-twin structure, observed by polarized-light microscopy, which consists of extensive β-spherulites in the core with α-spherulitic overgrowths. Recently, Menyhard et al.[61] comparatively investigated the nucleating efficiency and selectivity of some different β-nucleating agents. They showed that the efficiency and the selectivity of Ca-suberate and Ca-pimelate are extremely high in a wide concentration range, while NJ is highly efficient but not completely selective; i.e., α-iPP is always formed in its presence. The phenomena of double exothermic peaks in DSC crystallization traces largely depends on the concentration and type of β-nucleating agent.[32] In particular, the characteristics of the structure induced by NJ are determined by the dual nucleation process, i.e., the mechanism that triggers the growth of α- and β-phase simultaneously, and by the solubility of this nucleating agent, as well as by the thermal conditions during cooling and crystallization. Varga et al.[62] have shown that the lateral surface of the needle crystals of NJ acts as α-nucleating agent using polarized light microscopy. Because of the solubility and dual nucleating ability of NJ, a wide variety of supermolecular structures may form in its presence, such as an $\alpha\beta$-transcrystalline layer that develops on the lateral surface of the needle crystals of NJ, dendritic and microcrystalline structures, and a spectacular flowerlike agglomerate of α- and β-crystallites.

The rate of crystallization was analyzed using the values of $1/\tau_{0.1}$ as a representation of the global crystallization rate for each crystallization temperature. A pronounced change in this parameter was observed as the crystallization temperature increased, in other words, as the undercooling decreased (Figure 2). In particular, the incorporation of 0.05 wt % of NJ results in an obvious increment of the crystallization rate of iPP/IF-WS_2 nanocomposites, while the relative increase is less important and tends to stabilize at concentrations superior or equal to 0.25 wt % of NJ. Although the crystallization rate of iPP/IF-WS_2/NJ is lower than of iPP/NJ (0.1 wt %), it cannot be concluded that a synergetic nucleation effect exists to accelerate the crystallization of iPP. Indeed, the introduction of both a highly efficient β-NA and an active nanofiller with remarkably good α-nucleating ability into iPP may induce competitive growth between the α- and β-modifications.

The melting behavior of iPP nucleated with the different NA systems (individual and dual) was investigated by heating the isothermally crystallized samples at a heating rate of 5 °C/min, and the DSC heating thermograms are presented in Figure 3. It

dx.doi.org/10.1021/jp2099703 | J. Phys. Chem. B 2012, 116, 1788−1795

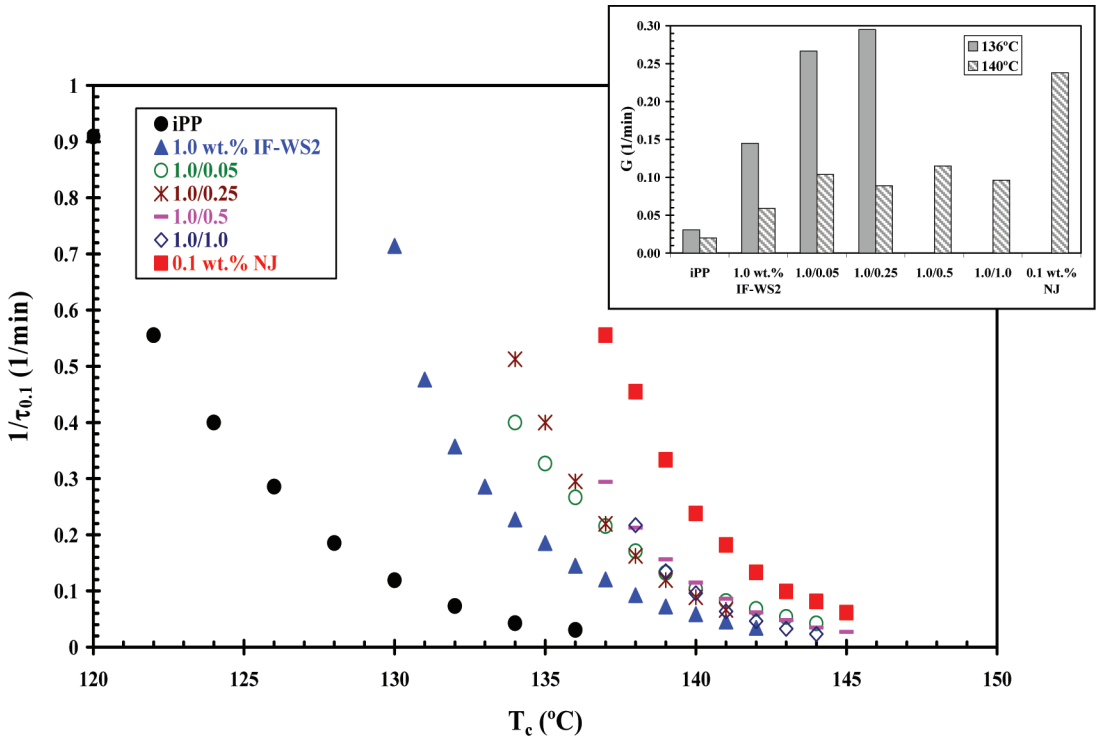

Figure 2. Variation of the rate of crystallization $(1/\tau_{0.1})$ with crystallization temperature (T_c) for iPP nucleated with dual α(IF-WS_2)/β(NJ) NAs and individual α or β NAs. Inset: the corresponding $1/\tau_{0.1}$ values for iPP systems obtained at values of T_c indicated.

is clear that the crystallization temperature has a significant effect on the melting behavior of the matrix material after isothermal crystallization. Figure 3a presents the melting behavior of isothermally crystallized iPP/IF-WS_2 (1.0 wt %) nanocomposite at different crystallization temperatures. The melting curve of iPP nucleated with 1.0 wt % of IF-WS_2 appears as two melting endotherms: a broad and poorly defined shoulder at lower temperatures and a well-defined peak at higher temperature. All melting temperatures shift to higher values with increasing T_c, suggesting the existence of partial size segregation of the crystals in the isothermally formed α-crystallites.[60] The smaller crystals generated the lower temperature shoulders, and the enthalpy contribution of the melting of the thicker more perfect crystals is contained in the higher temperature endotherm. However, a contribution from the melting−recrystallization−melting of more imperfect crystals cannot be ruled out.[63] The integration of the double endothermic peaks allowed the calculation of the crystallinity values of the α-form (Figure 3b), which appears to be independent of the crystallization temperature, having a value of $X_\alpha \sim 55\%$.

However, for the β-nucleated samples (Figure 3c), the melting behavior varies with the changes in the value of T_c. An endothermic peak containing the contribution of almost only β-form appearing at around 160 °C is observed in the melting curves of samples crystallized at relatively low T_c (~138−140 °C), and the relative content of the β-form (k_β) in the iPP/NJ(0.1 wt %) is >90% (Figure 3d). This confirms the preferred β-phase growth during the initial crystallization period. With increasing T_c, the endotherm corresponding to the α-form appeared and gradually intensified, indicating that an increasing contribution of the α-form developed during the isothermal crystallization process. A particular growth feature of the β-form is the transformation from metastable β-form into α-form.[4] During this transition α-nuclei are formed on the growing β-crystal front that results in the growth of α-spherulitic segments. This phenomenon results in characteristic $\beta\alpha$-twin structures that consist of a β-phase core with more or less α-spherulitic overgrowths. The kinetic precondition of the phase transition at the growing crystal fronts is that the growth rate of the new phase should be higher than that of the base crystal; otherwise, the nuclei corresponding to the new phase would be overgrown by the original crystal front. Compared with the formation of pure β-polypropylene, this transition has the lower and upper critical temperatures, $T(\alpha\beta) \sim 100$ °C and $T(\beta\alpha) \sim 140$ °C. Between these temperatures, the β-phase grows faster than the α-phase. In particular, a further increase in T_c in the range of $T_c > T(\beta\alpha)$ enhances the probability of $\beta-\alpha$ transitions that become predominant as the melting temperature of β-form is approached. However, in the present work, even at values of T_c up to 145 °C the endotherm associated with the melting of the β-form is still larger that that of the α-form, reflected in the calculated crystallinity values for these phases of $X_\beta \sim 62\%$ and $X_\alpha \sim 34\%$ (Figure 3d). These results suggest that the addition of NJ expanded the upper limit temperature for the formation of the β-modification, allowing the induction of the β-form over a broader T_c range than previously reported.

In the case of iPP nucleated by α(IF-WS_2)/β(NJ), the melting behavior subsequent to the isothermal crystallization process is strongly dependent not only on the crystallization temperature but also on the relative content of α- and β-NAs (Figure 3e−h). As an example, Figure 3e shows the melting thermograms of iPP nucleated with 1.0 wt % IF-WS_2 and 0.05 wt % NJ. It can be clearly seen that the melting peak of the β-phase is superimposed onto the two α-peaks in the melting curves of the sample crystallized below $T(\beta\alpha)$, at $T_c = 134$ °C. Indeed, the melting curves of the α-peaks very much resemble

dx.doi.org/10.1021/jp2099703 | J. Phys. Chem. B 2012, 116, 1788−1795

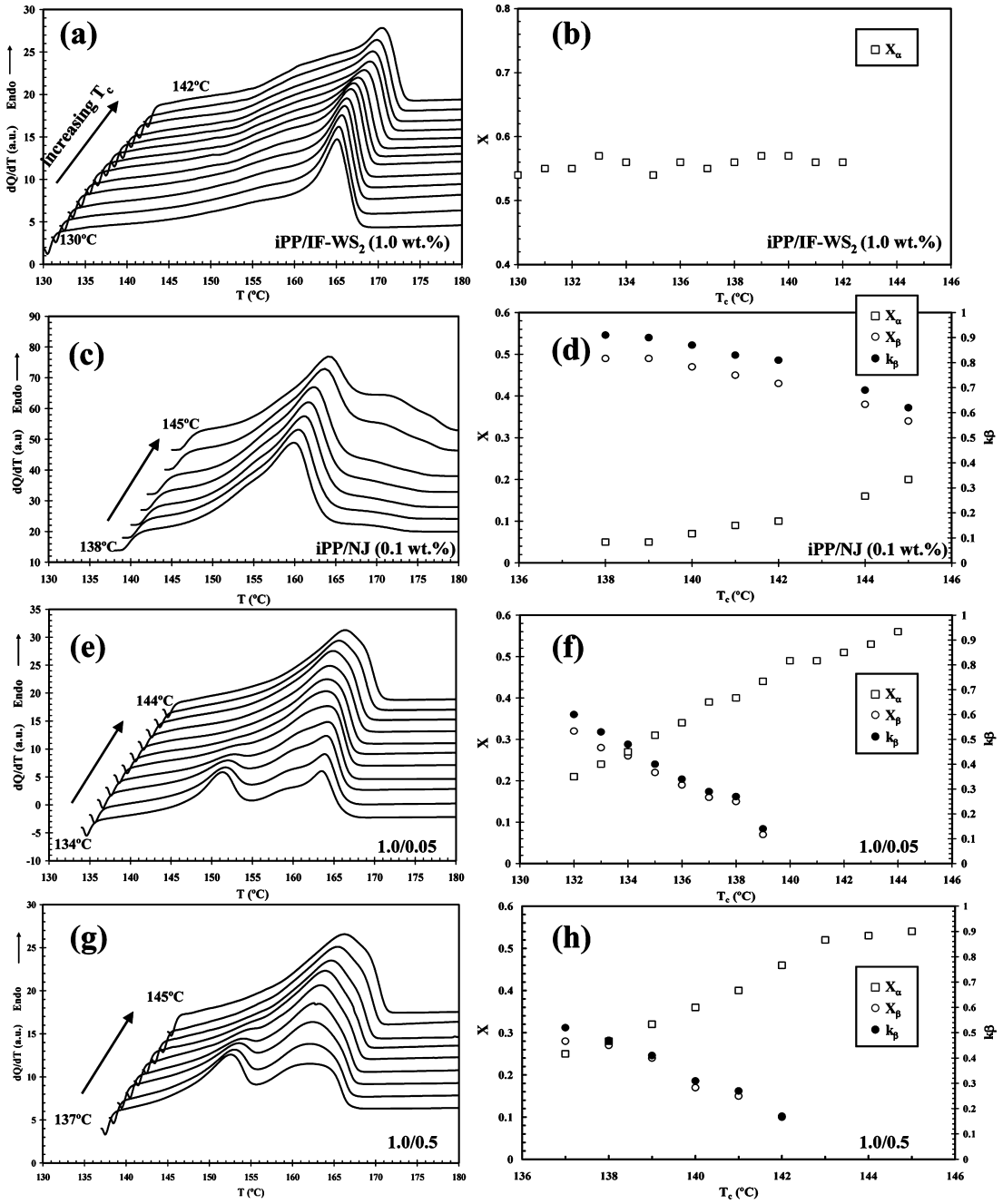

Figure 3. Melting behavior of iPP nucleated with dual α(IF-WS$_2$)/β(NJ) NAs and individual α- or β-NAs obtained at a heating rate of 5 °C/min after isothermal crystallization. Left panel shows the evolution of DSC melting thermograms of iPP systems with T_c, and right panel illustrates the corresponding crystallinity values of the α-form, X_α, and β-form, X_β, and the β-form content (k_β) calculated from eqs 1−3.

those observed for iPP/IF-WS$_2$ samples at high temperature. As T_c increased, the melting peak of the β-phase became less and less pronounced in accordance with the evolution of the values of both X_β and k_β (Figure 3f). If $T_c > T(\beta\alpha)$, the melting curves only contained peaks corresponding to the α-modifications, α_1 and α_2. However, it should be noticed that α_2 shoulder in these samples may be associated with the melting−recrystallization−melting of the α-phase crystals of lower size or perfection and fusion of those reorganized into the α-phase from the melting of unstable β-phase crystals during heating. In the same way, the system iPP/IF-WS$_2$(1.0 wt %)/NJ(0.5 wt %) presents a similar melting behavior to that of iPP/IF-WS$_2$(1.0 wt %)/NJ(0.05 wt %), also indicating the structural resemblance between the sample. But it should be noticed that the presence of NJ played a dominant role during the crystallization process until 138 °C, around 4 °C higher than that of the iPP nucleated with low NJ content such as 0.5 wt %, which can be appreciated from the evolution of both X_α and X_β shown in Figures 3f and 3h.

To further verify the influence of the NJ content on the evolution of the polymorphic behavior of iPP, a comparative analysis of the melting curves of iPP nucleated by individual and dual NAs is shown in Figure 4. As an example, Figure 4a illustrates the dependence of the melting endotherms of iPP that was isothermally crystallized at 138 °C as a function of composition. It can be clearly observed that the IF-WS$_2$/NJ

dx.doi.org/10.1021/jp2099703 | J. Phys. Chem. B 2012, 116, 1788−1795

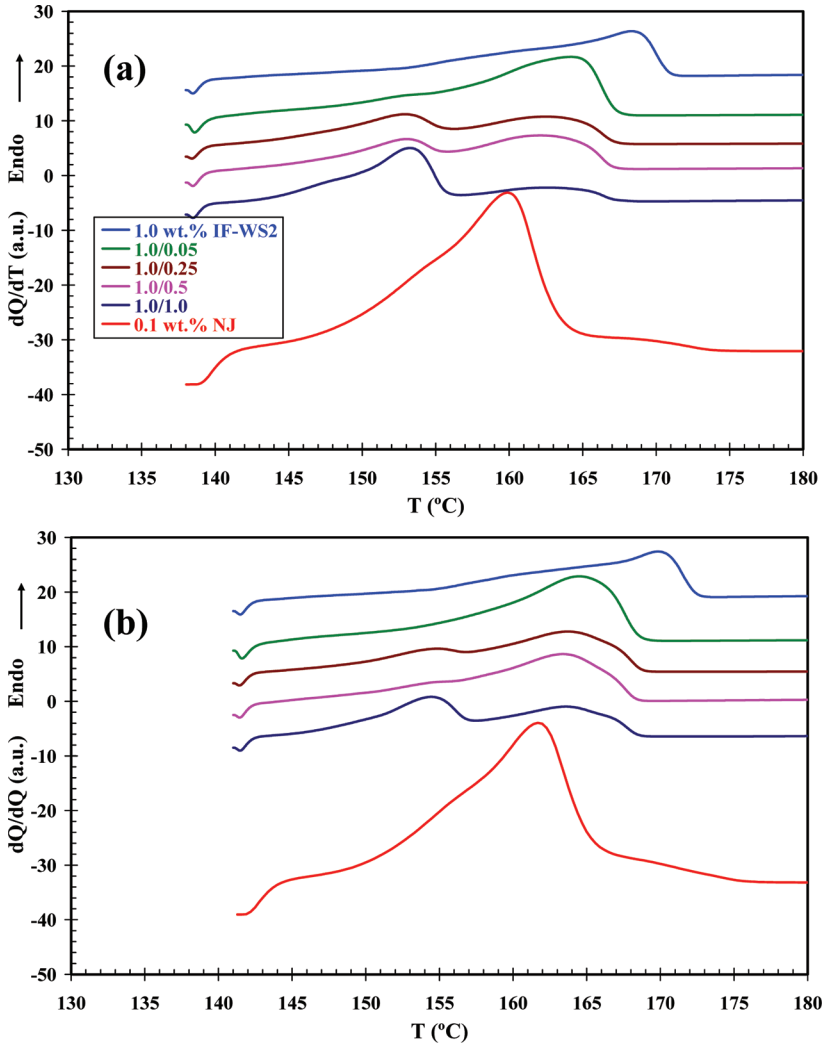

Figure 4. DSC melting thermograms for iPP nucleated with dual α(IF-WS_2)/β(NJ) NAs and individual α- or β-NAs obtained at a heating rate of 5 °C/min after isothermal crystallization at (a) 138 °C and (b) 141 °C.

concentration balance has an impact on the melting behavior of the iPP matrix, and the peak shape and melting temperatures of the iPP samples nucleated by the dual agent system progressively change with increasing NJ content. In particular, for the iPP/IF-WS_2/NJ samples the melting temperatures of the α- and β-phases do not reach the corresponding values obtained for iPP nucleated with the individual NAs, i.e., pure IF-WS_2 or pure NJ. Such behavior can be related again to the complex and strong growth competition between the α- and β-phases. In addition, the further increase of the crystallization temperature to 141 °C enhances the probability of $\beta-\alpha$ transformation, and consequently the formation of the β-crystal form becomes less and less pronounced in comparison with the formation of the predominant α-crystal form. This is in accord with the evolution of crystallinity values of the α-crystal form, X_α, and β-crystal form, X_β, as well as the variation of the relative content of β-crystals (k_β) with the crystallization temperature (Figure 5a–c). For the iPP samples nucleated by α(IF-WS_2)/β(NJ) the value of k_β decreases continuously with further increases in the relative IF-WS_2 content, indicating an effective adjustment of the polymorphic composition by the variation of the proportion of IF-WS_2/NJ (Figure 5c). Correspondingly, the change of X_β as a function of NJ content is the same as that of k_β for all types of samples (Figure 5b). Obviously, the introduction of both highly efficient nucleating agents into iPP may induce competitive growth between the α- and β-modifications (Figure 5a,b). By altering the nucleating ability of the α-NA component or the β-NA component, the formation of a particular crystalline modification can be depressed or promoted, resulting in a significant change in the polymorphic behavior. As a routine consideration, the β-nucleating ability of NJ should be depressed more and more with the increasing relative α-NA (IF-WS_2) content. These findings are very useful for the development of new strategies for the preparation of iPP nanocomposites with tuned mechanical properties via the addition of dual nucleating systems containing α(IF-WS_2)- and β(BJ)-nucleating agents.

4. CONCLUSIONS

The isothermal crystallization process of dual α(IF-WS_2)/β(NJ) nucleated iPP strongly depends on both the nucleating agent concentration and the crystallization temperature. In iPP/IF-WS_2/NJ systems, the addition of β(NJ)-nucleating agent exerted a significant effect on the rate of crystallization ($1/\tau_{0.1}$) of iPP that was influenced, in turn, by the crystallization temperature. The value of $1/\tau_{0.1}$ for iPP/IF-WS_2 at a particular crystallization temperature continues to rise with the addition of NJ, tending to stabilize at concentrations superior or equal to

dx.doi.org/10.1021/jp2099703 | J. Phys. Chem. B 2012, 116, 1788–1795

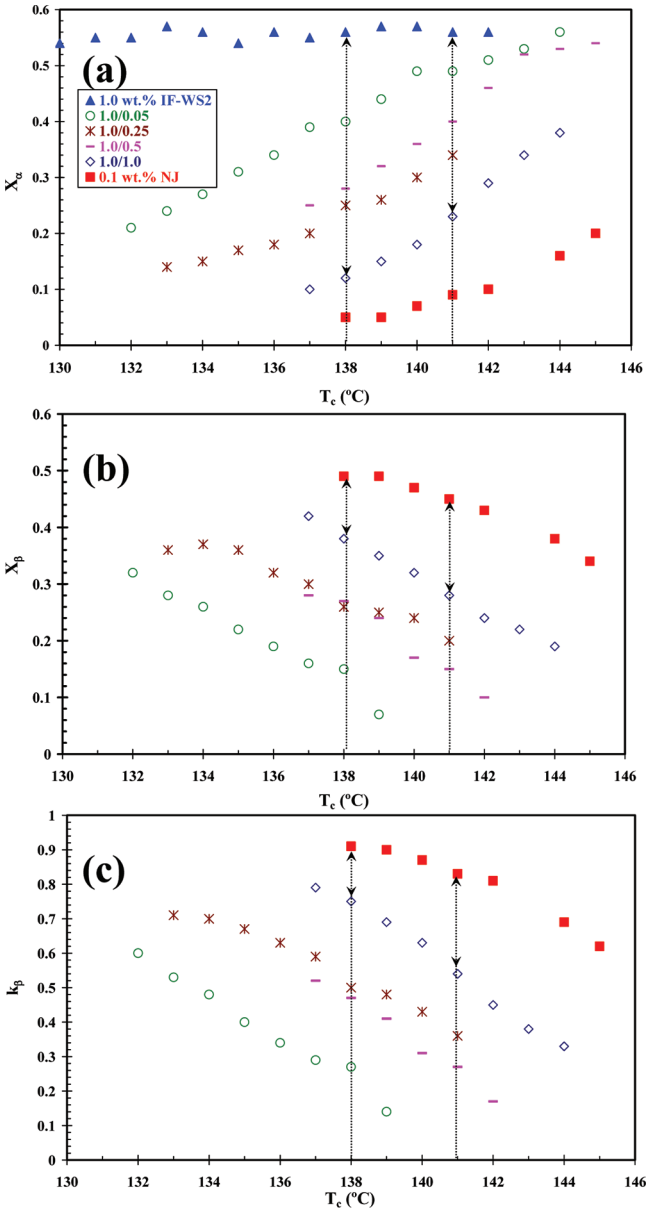

Figure 5. Variation of the crystallinity values of the (a) α-crystal form, X_α, and (b) β-crystal form, X_β, as well as (c) the variation of the relative content of β-crystals (k_β) with the crystallization temperature for the iPP systems indicated.

0.25 wt % of the β(NJ)-nucleating agent. The kinetic study of isothermal crystallization also showed that IF-WS_2/NJ was more effective than IF-WS_2 in accelerating the crystallization rate of iPP. However, the best enhancement of the crystallization rate of iPP was only achieved by the addition of the individual NJ. In particular, when iPP was nucleated with a low amount of NJ (0.1 wt %), the crystallization rate of iPP is remarkably increased, and a unique crystallization behavior is manifested by doubling of the crystallization exotherms. This phenomenon was not detected in neat iPP or in iPP/IF-WS_2/NJ systems and was ascribed to separated growth of the α- and β-phases. Similarly, the melting behavior of iPP/IF-WS_2 depends strongly on the NJ content. The shape and melting peaks of iPP samples nucleated by dual α(IF-WS_2)/β(NJ) systems progressively change with increasing NJ content. When $T_c > T(\beta-\alpha)$, the melting curves contain only the α_1- and α_2-modifications, indicating a complex and strong growth competition phenomenon between the α- and β-phases that correlates with the evolution of crystallinity values of the α- and β-crystal form as well as the relative content of β-crystals with the crystallization temperature.

AUTHOR INFORMATION

Corresponding Author

*E-mail: mnaffakh@ictp.csic.es.

Notes

The authors declare no competing financial interest.

ACKNOWLEDGMENTS

This work was supported by the Spanish Ministry of Science and Innovation, MICINN (Project MAT2010-21070-C02-01). Dr. M. Naffakh expresses thanks to the Consejo Superior de Investigaciones Científicas (CSIC) for an Intramural Research Fellowship (under Project 201160E003).

REFERENCES

(1) Grein, C. *Adv. Polym. Sci.* **2005**, *188*, 43−104.
(2) Thierry, A.; Straupé, C.; Wittmann, J. C.; Lotz, B. *Macromol. Symp.* **2006**, *241*, 103−110.
(3) Libster, D.; Aserin, A.; Garti, N. *Polym. Adv. Technol.* **2007**, *18*, 685−695.
(4) Varga, J. *J. Macromol Sci., Part B: Phys.* **2002**, *41*, 1121−1171.
(5) Gahleitner, M.; Grein, C.; Kheirandish, S.; Wolfschwenger, J. *Int. Polym. Proc.* **2011**, *16* (1), 2−20.
(6) Mauritz, K. A.; Baer, E.; Hopfinger, A. J. *J. Polym. Sci., Macromol. Rev.* **1978**, *13*, 1−61.
(7) Vidotto, G.; Levy, D.; Kovacs, A. J. *Kolloid Z. Z. Polym.* **1969**, *230*, 289−305.
(8) Legras, R.; Mercier, J. P.; Nield, E. *Nature* **1983**, *304*, 432−434.
(9) Manias, E.; Touny, A.; Wu, L.; Strawhecker, K.; Lu, B.; Chung, T. C. *Chem. Mater.* **2001**, *13*, 3516−3523.
(10) Moniruzzaman, M.; Winey, K. I. *Macromolecules* **2006**, *39*, 5194−5205.
(11) Winey, K. L.; Vaia, R. A. *MRS Bull.* **2007**, *32*, 314−322.
(12) Padden, F. J. Jr.; Keith, H. D. *J. Appl. Phys.* **1959**, *30*, 1479−1484.
(13) Keith, H. D.; Padden, F. J. Jr.; Walter, N. M.; Wyckoff, H. W. *J. Appl. Phys.* **1959**, *30*, 1485−1488.
(14) Brückner, S.; Meille, S. V.; Petraccone, V.; Pirozzi, B. *Prog. Polym. Sci.* **1991**, *16*, 361−404.
(15) Lotz, B.; Wittmann, J. C.; Lovinger, A. J. *Polymer* **1996**, *37*, 4979−4992.
(16) Auriemma, F.; De Rosa, C.; Corradini, P. *Adv. Polym. Sci.* **2005**, *181*, 1−74.
(17) Androsch, R.; Di Lorenzo, M. L.; Schick, C.; Wunderlich, B. *Polymer* **2010**, *51*, 4639−4662.
(18) Fujiwara, Y. *Colloid Polym. Sci.* **1975**, *253*, 273−283.
(19) Lovinger, A. J.; Chua, J. O.; Gryte, C. C. *J. Polym. Sci. Polym. Phys.* **1977**, *15*, 641−656.
(20) Leugering, H. J.; Kirsch, G. *Angew. Makromol. Chem.* **1973**, *33*, 17−23.
(21) Varga, J. *Angew. Makromol. Chem.* **1983**, *112*, 191−203.
(22) Varga, J.; Karger-Kocsis, J. *J. Polym. Sci., Part B: Polym. Phys.* **1996**, *34*, 657−670.
(23) Somani, R. H.; Hsiao, B. S.; Nogales, A.; Fruitwala, H.; Srinivas, S.; Tsou, A. H. *Macromolecules* **2001**, *34*, 5902−5909.
(24) Chen, Y. H.; Mao, Y. M.; Li, Z. M.; Hsiao, B. S. *Macromolecules* **2010**, *43*, 6760−6771.
(25) Leugering, H. J. *Makromol. Chem.* **1967**, *109*, 204−216.
(26) Marco, C.; Ellis, G.; Gómez, M. A.; Arribas, J. M. *J. Appl. Polym. Sci.* **2002**, *86*, 531−539.

(27) Blomenhofer, M.; Ganzleben, S.; Hanft, D.; Schmidt, H. W. *Macromolecules* **2005**, *38*, 3688−3695.
(28) Varga, J.; Mudra, I.; Ehrenstein, G. W. *J. Appl. Polym. Sci.* **1999**, *74*, 2357−2368.
(29) Cui, L.; Zhang, Y.; Zhang, Y. *J. Polym. Sci., Part B: Polym. Phys.* **2006**, *44*, 3288−3303.
(30) Vychopnová, J.; Habrová, V.; Obadal, M.; Cermák, R.; Cabla, R. *J. Therm. Anal. Calorim.* **2006**, *86*, 687−691.
(31) Zhang, Y. F. *J. Macromol. Sci., Part B: Phys.* **2008**, *47*, 891−899.
(32) Xiao, W.; Wu, P.; Feng, J. *J. Appl. Polym. Sci.* **2008**, *108*, 3370−3379.
(33) Raka, L.; Sorrentino, A.; Bogoeva-Gaceva, G. *J. Polym. Sci., Polym. Phys.* **2010**, *48*, 1927−1938.
(34) Varga, J.; Stoll, K.; Menyhárd, A.; Horváth, Z. *J. Appl. Polym. Sci.* **2011**, *121*, 1469−1480.
(35) Jacoby, P.; Bersted, B. H.; Kissel, W. J.; Smith, C. E. *J. Polym. Sci., Part B: Polym. Phys.* **1986**, *24*, 461−491.
(36) Tjong, S. C.; Shen, J. S.; Li, R. K. Y. *Polym. Eng. Sci.* **1996**, *36*, 100−105.
(37) Karger-Kocsis, J.; Varga, J. *J. Appl. Polym. Sci.* **1996**, *62*, 291−300.
(38) Tordjeman, Ph.; Robert, C.; Marin, G.; Gerard, P. *Eur. Phys. J. E* **2001**, *4*, 459−465.
(39) Marco, C.; Gómez, M. A.; Ellis, G.; Arribas, J. M. *Recent Res. Dev. Appl. Polym. Sci.* **2002**, *1*, 587−610.
(40) Ferro, D. R.; Meille, S. V.; Brckner, S. *Macromolecules* **1998**, *31*, 6926−6934.
(41) Brckner, S.; Meille, S. V. *Nature* **1989**, *340*, 455−457.
(42) Meille, S. V.; Brckner, S.; Porzio, W. *Macromolecules* **1990**, *23*, 4114−4121.
(43) Jin, Y.; Hiltner, A.; Baer, E.; Masirek, R.; Piorkowska, E.; Galeski, A. *J. Polym. Sci., Part B: Polym. Phys.* **2006**, *44*, 1795−1803.
(44) Galli, P.; Vecellio, G. *Prog. Polym. Sci.* **2001**, *26*, 1287−1336.
(45) Bucknall, C. B.; Soares, V. L. P.; Yang, H. H.; Zhang, X. C. *Macromol. Symp.* **1996**, *101*, 265−271.
(46) Karnani, R.; Krishnan, M.; Narayan, R. *Polym. Eng. Sci.* **1997**, *37*, 476−483.
(47) Thio, Y. S.; Argon, A. S.; Cohen, R. E.; Weinberg, M. *Polymer* **2002**, *43*, 3661−3674.
(48) Zhang, Y. F.; Xin., Z. *J. Polym. Sci., Part B: Polym. Phys.* **2007**, *45*, 590−596.
(49) Zhang, Y. F. *J. Polym. Sci., Part B: Polym. Phys.* **2008**, *46*, 911−916.
(50) Bai, H.; Wang, Y.; Zhang, Q.; Liu, L.; Zhou, Z. *J. Appl. Polym. Sci.* **2009**, *111*, 1624−1637.
(51) Zhao, S.; Xin, Z. *J. Polym. Sci., Part B: Polym. Phys.* **2010**, *48*, 653−655.
(52) Zhang, N.; Zhang, Q.; Wang, K. *J. Therm. Anal. Calorim.* **2011**, DOI: 10.1007/s10973-011-1637-z.
(53) Chen, H.; Wang, M.; Lin, Y.; Chan, C. M.; Wu, J. *J. Appl. Polym. Sci.* **2007**, *106*, 3409−3416.
(54) Naffakh, M.; Martín, Z.; Fanegas, N.; Marco, C.; Gómez, M. A.; Jiménez, I. *J. Polym. Sci., Part B: Polym. Phys.* **2007**, *45*, 2309−2321.
(55) Naffakh, M.; Marco, C.; Ellis, G. *J. Phys. Chem. B* **2011**, *115*, 10836−10843.
(56) Marco, C.; Ellis, G.; Gómez, M. A.; Arribas, J. M. *J. Appl. Polym. Sci.* **2002**, *84*, 1669−1679.
(57) Marco, C.; Ellis, G.; Gómez, M. A.; Arribas, J. M. *J. Appl. Polym. Sci.* **2002**, *84*, 2440−2450.
(58) Li, X.; Cheung, W. L. *Polymer* **1998**, *39*, 6935−6940.
(59) Li, J. X.; Cheung, W. L.; Demin, J. *Polymer* **1999**, *40*, 1219−1222.
(60) Naffakh, M.; Martín, Z.; Marco, C.; Gómez, M. A.; Jiménez. *Thermochim. Acta* **2008**, *472*, 11−16.
(61) Menyhárd, A.; Varga, J.; Molnar, G. *J. Therm. Anal. Calorim.* **2006**, *83*, 625−630.
(62) Varga, J.; Menyhárd, A. *Macromolecules* **2007**, *40*, 2422−2431.
(63) Marco, C.; Ellis, G.; Gómez, M. A.; Arribas, J. M. *J. Appl. Polym. Sci.* **2003**, *88*, 2261−2274.